Environmental Science Nano

ROYAL SOCIETY OF CHEMISTRY

PAPER

View Article Online
View Journal | View Issue

Check for updates

Cite this: *Environ. Sci.: Nano*, 2022, **9**, 4585

Nano and submicron fluorescent polystyrene particles internalization and translocation in seedlings of *Cichorium endivia* L.†

Simonetta Muccifora, [a] Lucia Giorgetti, *[b] Maddalena Corsini, [c] Giuseppe Di Florio [c] and Lorenza Bellani [ab]

Contamination by plastics is one of the major causes of pollution of the terrestrial environment. Fragmentation of plastics into micro and nano particles may result in negative interactions between polymers and terrestrial ecosystems. The effects of nano (20 nm) and submicron (200 nm) fluorescent polystyrene (PS) particles, at different concentrations (0.01, 0.1, 1 g L^{-1}), were analysed on chicory plant (*Cichorium endivia* L.), considering the following endpoints: germination percentage and seedling development after 7 and 14 days exposure; genotoxic effects; polyphenols and photosynthetic pigments content, antioxidant activity; absorption and translocation of PS particles in the seedling tissues. The results indicated no negative effects on germination of both PS particles' sizes at any concentration; seedlings elongation was affected by 1 g L^{-1} of 20 nm PS after 7 days exposure. Cytological analysis revealed no mitotic activity inhibition, but an uprising of chromosomal abnormalities in all treatments. Interestingly, photosynthetic pigments always increased after PS exposure. Seedlings treated with 20 nm PS showed intense fluorescence in the roots of 7 days and in the shoots of 14 days, while 200 nm PS treated seedlings exhibited low fluorescence. Electron microscopy and infrared spectroscopy confirmed 20 nm PS internalization and transport inside the plant tissue and a reduced presence of 200 nm PS. These results suggest the importance not only of particle size in plastic internalization in plant tissues, but also of cytological damages induced by particles too large to be bioaccumulated. From both aspects, consequences may arise for plant fitness, food safety and human health.

Received 6th August 2022,
Accepted 3rd November 2022

DOI: 10.1039/d2en00732k

rsc.li/es-nano

Environmental significance

Plastic contamination is one of the major concerns in environment protection, for its persistence in the environment and effects on living organisms. Many studies are examining the effects of plastics on plants, to ascertain the possible entry inside the food chain of micro and nanoplastics. Our study, based on the use of fluorescent 20 nm and 200 nm polystyrene particles, evidenced the uptake and translocation of particles in chicory seedlings by fluorescent and electron microscopy and infrared spectroscopy analysis, and the consequent effects determined at biochemical, ultrastructural and cytogenetic levels. Our findings indicated the relevance of size and concentration of plastics particles for plants contamination in the environment and enriched the recent knowledge shedding light into plastic interactions with ecosystems.

1. Introduction

In the last century, the global introduction of plastic materials in all industrial and domestic fields, in agriculture, in pharmaceuticals, in cosmetics, *etc.*, resulted in an exponential increase in plastics production, improving the technologies and lifestyle of all human beings. In 2019, plastics production reached 370 million tonnes with about 58 million tonnes produced in Europe.[1] Unfortunately, the high technology and financial investments to create ever more performing plastic products have not been accompanied by adequate and in time practices to avoid the indiscriminate discharge and contamination in the environment. Awareness of the environmental impact of plastic waste is relatively recent and its removal and containment in terrestrial and aquatic ecosystems represents one of the greatest and urgent challenges of the new century.[1] The major concern is that

[a] *Department of Life Sciences, University of Siena, Siena, Italy*
[b] *Institute of Agricultural Biology and Biotechnology, (IBBA-CNR), Pisa, Italy. E-mail: lucia.giorgett@ibba.cnr.it*
[c] *Department of Biotechnology, Chemistry and Pharmacy, University of Siena, Siena, Italy*

† Electronic supplementary information (ESI) available. See DOI: https://doi.org/10.1039/d2en00732k

plastic polymers persist in the environment for many decades and undergo aging phenomena due to physical and chemical events, producing smaller fragments up to the size of microplastics (less than 5 mm) and nanoplastics (less than 100 nm in all the three dimensions).[2] The microplastics generated in this way are defined as secondary microplastics by distinction from the primary ones, directly introduced into the environment mainly through cosmetics or as air-blasting media for cleaning rust and paint off machinery and boat hulls.[3,4]

Many studies have focused on micro and nanoplastic contamination in order to determine their effects on living beings at different levels of the food chain, firstly in the marine environments and only very recently in terrestrial ecosystems and plants.[5] It should be emphasized that the results of the environmental monitoring studies have revealed that the terrestrial contamination can be much higher than the aquatic one and that agricultural soils can also accumulate micro and nanoplastics, by the use of fertilizing sludge and plastic mulching.[6]

Independently from the source of micro and nanoplastics, the particles dispersed in the environment can be directly ingested/inhaled or taken up by aquatic and terrestrial organisms, or absorbed by plants, thus entering the food chain. For these reasons they represent a real problem for the quality of the environment and for plant food/feed products for human and animal nutrition.[7] In fact, the possible disturbances of plastics to the plant cell or to plant organism physiology and to the microbial ecology of soil might affect the plant life cycle, the nutritional properties of plant edible parts, and the whole ecosystems.[7,8] In particular, it is of great interest to study the intake of plastics by edible plants and edible portions of plants, to evaluate the extent of their transmission to the food chain. Recent work on mung bean grown in soil spiked with nanoplastics at 10 and 100 mg kg^{-1}, reports toxic effects and accumulation in plants, and subsequent effects on terrestrial snails after leaf ingestion.[8] The risks connected with the micro and nanoplastics contamination of terrestrial plants and aquatic macrophytes are scarcely known, but the ability of plants to adsorb and/or internalise micro- or nanoplastics has already been highlighted, the effects depending on the physical characteristics and the chemical composition of the plastic polymer.[9]

Microplastics can inhibit seed imbibition[10] or, accumulating near the root tip of terrestrial plants, they can alter water imbibition and nutrient absorption through the blockage of cell wall pores.[11]

Direct effects of plastic micro and nanoparticles on plant physiology at the vegetative and reproductive stages were observed.[12–16] In addition, plastics can alter abiotic and biotic soil properties and affect root colonization by arbuscular mycorrhizal fungi (AMF) and by non-AMF and can indirectly influence plant performance.[17]

Most studies reported that micro and nanoplastics uptake by plants may depend on both the size and the shape of materials, on the aggregation tendency and the ability to alter the pore diameter of the cell wall, acting on the dynamic behaviour of its components.[16,18] Among plastics, polystyrene (PS) represents one of the most commonly found polymer in terrestrial ecosystems and its particles have been selected to study the effects of plastic materials, at nano and microscale on different living systems.[19] Oliveri Conti *et al.*[20] demonstrated the presence of micro and nanoparticles of PS in vegetables and fruits purchased from local markets, although it was not evidenced by which path these particles would accumulate in the plant edible tissues.

Since *Cichorium endivia* (chicory) is largely used in human diet for its beneficial effects on health, due to the antibacterial activity,[21] anti-inflammatory,[22] antioxidant, hepatoprotective and antidiabetic[23] functions, in the present study chicory was used as model plant to test the effects of 20 nm and 200 nm PS particles. The choice of the concentrations (0.01 g L^{-1}, 0.1 g L^{-1} and 1 g L^{-1}) derived from environmentally realistic concentrations.[8] In marine ecosystems relevant concentration proposed for nano PS as pollutant was <15 μg L^{-1},[24] in soil, the discrimination and the identification of nanoplastics is very difficult for the formation of nanoaggregates and the interaction with soil components[25] and it was estimated to be at higher levels in respect to marine environment, up to a factor of four.[26]

The peculiarity of this work arises from the synergic use of Transmission Electron Microscopy and fluorescence microscopy, that can evidence the internalization of PS particles, and Fourier-Transform Infrared Spectroscopy in Attenuated Total Reflection mode,[27] that characterizes the PS particles, in terms of chemical composition and purity, and their presence inside plant samples.

The aim of the present study was to analyze the effects of different concentrations of PS particles on the physiology of germination of *C. endivia* seeds, on genotoxicity and on the possible absorption and translocation within the seedlings, together with the possible impact on antioxidant activity and on phytochemical compounds and photosynthetic pigments content.

2. Materials and methods

2.1 Polystyrene particles' characterization

Polystyrene nanoparticles (nPS) of 20 nm lot 231257, R25 Fluoro Max color – dyed microsphere suspension, catalogue number 10526245, and submicron particles (smPS) of 200 nm, lot 232486, R200 Fluoro Max color – dyed microsphere suspension, catalogue number 10200035, dyed with red fluorescent dyes, were purchased by Thermofisher. Fluorescent dye – a proprietary formulation – is incorporated into polymer matrix. Particles, packaged in deionized water (1% suspension) with trace amounts of surfactant, a sodium dodecyl sulfate (SDS) derivative with concentration of 0.1% non-beads solids for smPS particles and 0.51% non-beads solids for nPS particles, and preservative sodium azide

<0.05% to inhibit aggregation and promote stability, have a refractive index of 1.59 and a density of 1.06 g cm^{-3}. The spectral properties of the dye are: colour = red; excitation maxima in nm = 542 (green); emission maxima in nm = 612 (red). Stokes shift in nm = 70.

2.2 Plant material and seed germination

Commercial seeds of *Cichorium endivia* var. riccia cuor d'oro were purchased (lot n. QC0154, harvest of 2020) and stored at −20 °C until use.

Glass Petri dishes of 6 cm diameter were used in the germination experiments, to avoid possible contamination by the commonly used polystyrene plastic dishes. Twenty seeds were sown in each dish, kept in the dark at 22.5 ± 1 °C for 7 days, then exposed to light for other 7 days. The seeds were sown in distilled water (control) and in 0.01, 0.1, 1 g L^{-1} suspension in water of both size particles. The PS suspensions were sonicated before use for 5 min in an Esterline Angus sonicator.

Three replicates were prepared for the control and for each treatment. The experiment was repeated three times.

At 7 and 14 days the percentage of germination (% G) and the length of root and shoot were separately evaluated and expressed in cm. The seeds were considered germinated when the length of the radicle was at least equal to their diameter. The % G is represented by the percentage of seeds germinated on the total number of seeds in the plate.

Seed germination and root–shoot elongation were observed with a Leica Wild M 10 stereo microscope.

All seedling before use were thoroughly washed in distilled water and gently dried to remove PS particles eventually sticked onto surfaces.

Seedlings were surface dried and weighed to determine fresh weight (FW), then oven dried at 103 °C for 18 h, and weighed again, for dry weight (DW) determination.

2.3 Attenuated Total Reflection (ATR) Fourier-Transform Infrared Spectroscopy (FTIR)

ATR infrared spectra of stock nPS and smPS particles were collected by dropping 4 μl of suspension onto a glass coverslip and allowing the solvent to evaporate.

Control and 1 g L^{-1} nPS and smPS particles treated seedlings at 14 days were homogenated in distilled water. An extraction protocol with organic solvent was developed, with the aim of preparing suitable samples for ATR measurements. In detail, for polymer extraction, 1 mL of homogenate was added with 1 mL of diethyl ether (analytical reagent grade) and vortexed for 5 min. The solution was let to settle for 30 min, then the organic solvent was collected. The procedure was repeated and the organic phase, collected from the second extraction, was added to the first. After the sedimentation, the organic and aqueous phases were separated by a thick interface, rich in specks from homogenate. Few drops of the three phases were placed on coverslip glasses and the solvents let to evaporate. Coverslips were subsequently placed on the ATR diamond crystal and clamped using a pressure gauge to obtain an accurate coverage of the crystal. FTIR-ATR spectra were collected in the 650–4000 cm^{-1} range with an Agilent Cary 630 FTIR spectrometer, equipped with a type IIa synthetic diamond crystal, single-reflection ATR accessory. All spectra and background spectra were recorded with 128 scans at 4 cm^{-1} resolution. To ensure that no spectral modifications occurred to polystyrene following the extraction procedure, the same experimental protocol was applied to nPS and smPS stock suspensions.

2.4 Transmission Electron Microscope (TEM)

Morphology and size of both the PS particles were characterized by TEM placing a drop (10 μl) of 1 g L^{-1} suspension on grids covered by formvar, allowed to settle, dried, and observed under a FEI Technai TEM at 100 kV. The particles dimensions were evaluated by the ImageJ program (ImageJ 1.52a, National Institutes of Health, USA, **https://imagej.nih.gov/ij**) by measuring the diameters of at least 100 particles from at least 4 different TEM images.[16]

For TEM observations, small cubes of control and 1 g L^{-1} nPS and smPS treated roots and shoots of 14 days, were pre-fixed in Karnovsky solution,[28] post-fixed in osmium tetroxide, dehydrated and embedded in Epon 812-Araldite A/M mixture. Thin sections were stained with uranyl acetate and lead citrate. Isolated PS particles and root and shoot sections were observed under TEM.

2.5 Cytogenetic analysis

Ten roots for control and each treatment were sampled after 5 days, fixed in ethanol/glacial acetic acid (3 : 1 v/v) overnight and stained following Feulgen stain procedure.[16] 1000 nuclei for each slide with five replicates for each treatment were randomly analysed by light microscope. Mitotic activity was expressed as mitotic index (MI, number of mitosis per 100 nuclei) to estimate the levels of cytotoxicity of the treatments. Mitotic aberrations (MA, number of aberrations per 100 nuclei) were determined for the genotoxicity analysis of the treatments. The cytological aberrations included mainly chromosomal bridges and fragments, lagging chromosomes, c-metaphases and disturbed anaphases in dividing cells.

2.6 Imaging of fluorescent polystyrene in seedlings

Seedlings control and treated for 7 and 14 days were rinsed in distilled water, placed on a glass slide, kept hydrated and covered with a coverslip prior to be observed under a Leika Fluorescent microscope equipped with a filter set: excitation 465–495 nm, emission 515–555 nm. Images were acquired by an AXIOCAM 5 photocamera.

2.7 Preparation of seedling extracts

Seedlings from each sample were placed in tubes with 80% ethanol solution, homogenized with Ultra Turrax T10, IKA

Works, at 4 °C, extracted for 3 h and centrifuged with Eppendorf Minispin at 927 RCF for 15 min. After collection of the supernatant, the pellet was resuspended, extracted for 24 h and centrifuged again for 15 min. Supernatants from both extractions were put together to reach a final concentration of 10% Wv and stored at −20 °C until use.

2.8 Determination of phytochemicals and pigments

The determination of total polyphenols (TPC) was performed following the method of Singleton and Rossi.[29] A solution of Folin–Ciocalteu was prepared in a 1 : 5 ratio in distilled water. 33 μl of extract were added to 1 ml of this solution and incubated for 6 min. Then, 666 μl of sodium carbonate solution (Na_2CO_3) 20% in distilled water were added in a progressive manner, stirred with Vortex and left at room temperature (RT) for 60 min. The absorbance was determined at 760 nm wavelength against a blank, with a spectrophotometer Varian Cary® 50 UV-vis spectrophotometer. For the blank, the extract was replaced by 80% ethanol. The TPC was estimated through the calibration curve of gallic acid and expressed as mg of gallic acid equivalent (mg GAE g^{-1} DW) of each extract.

The determination of total flavonoids (TFC) followed the colorimetric method of Heimler *et al.*:[30] 150 μl of extract were added to 45 μl of 5% sodium nitrite ($NaNO_2$) and 600 μl of distilled water. The solution was incubated at RT for 5 min. Then, 45 μl of 10% aluminium chloride ($AlCl_3$) were added and after incubation at RT for 6 min, 300 μl of 1 M sodium hydroxide (NaOH) and 360 μl of distilled water were added. After 5 min the absorbance was read with the spectrophotometer at 510 nm wavelength against a blank. The TFC was estimated through the calibration curve of quercetin and expressed as mg of quercetin equivalent (mg QE g^{-1} DW) of each extract.

Antioxidant activity was determined by the method of Boudjou *et al.*[31] A solution of 60 μM 2,2-diphenyl-1-picrylhydrazyl ($DPPH^{\bullet}$) (1950 μl) in MetOH was mixed with 50 μl of extract, vortexed and incubated at 25 °C in the dark for 60 min. Absorbance at 517 nm was measured against MetOH as a blank. As reference, 50 μl of EtOH were used instead of extract. Antiradical activity (ARA) was expressed as percentage inhibition of the $DPPH^{\bullet}$ radical, by the equation:

$$\mathrm{ARA} = 100\left(1 - \frac{\mathrm{Abs_{sample}}}{\mathrm{Abs_{reference}}}\right) \quad (1)$$

with Abs being the absorbance.

Chlorophylls (chl) and carotenoids (car) content was estimated following the method of Lichtenthaler.[32] In particular, 200 mg of leaves were homogenized in 6 ml of 80% acetone and centrifuged at 4 °C for 5 min at 2200 RFC. The supernatant was collected, the pellet resuspended in 6 ml of acetone and left to extract at 4 °C in the dark for 15 min. After centrifugation at 2200 RFC for 10 min at 4 °C, the two supernatants were combined and centrifuged again for 5 min in order to remove any suspended particles. The pigments were read at 663, 645 and 470 nm and the content of chl and car was obtained from the following formulas:

$$\mathrm{Chl_a} = (12.7\mathrm{Abs_{663nm}} - 2.69\mathrm{Abs_{645nm}})\frac{V_{\mathrm{FSN}}}{1000\mathrm{FW}} \quad (2)$$

$$\mathrm{Chl_b} = (22.9\mathrm{Abs_{645nm}} - 4.68\mathrm{Abs_{663nm}})\frac{V_{\mathrm{FSN}}}{1000\mathrm{FW}} \quad (3)$$

$$\mathrm{Chl_{tot}} = (20.2\mathrm{Abs_{645nm}} + 8.02\mathrm{Abs_{663nm}})\frac{V_{\mathrm{FSN}}}{1000\mathrm{FW}} \quad (4)$$

$$\mathrm{Car} = \frac{1000\mathrm{Abs_{470}} - 1.82\mathrm{Chl_a} - 85.02\mathrm{Chl_b}}{198} \cdot \frac{V_{\mathrm{FSN}}}{1000\mathrm{FW}} \quad (5)$$

V_{FSN} is the final supernatant volume and fresh weight (FW) is in grams.

Chlorophylls and carotenoid contents were expressed as mg g^{-1} DW.

2.9 Statistical analysis

Statistical analysis was performed using the Statistica package (StatSoft) version 6.0. All results are expressed as the arithmetic mean of three independent experiments ± standard deviation. Effects of PS particles for different factors, size and concentrations and their interactions were analyzed by ANOVA method. When the interactions between factors resulted significant, a *post-hoc* Tukey HSD test (Tukey honestly significant difference) was performed. Different letters indicate significative differences among means at $p \leq 0.05$ for the two times considered.

3. Results and discussion

3.1 Polystyrene particles characterization

Under TEM, the nPS particles presented an uneven roundish shape, while the smPS had regular round shape. PS particles size was grouped in frequency classes for size distribution (Fig. S1†). For nPS, the 65% of the particles had diameter minor than 20 nm, and the most represented frequency class (57%) had diameter 16–20 nm (Fig. S1a†). For smPS the 91% of the particles had diameter minor than 200 nm and the most represented frequency class (50%) had diameter 191–200 nm (Fig. S1b†). Furthermore, dynamic light scattering analysis has been carried out to characterize particles suspensions (Table S1†). The *z*-average for nPS was found to be 20 nm and for smPS 167 nm, while ζ-potential was, respectively, −40 mV and −60 mV.

The ATR-FTIR spectra of both size PS particles is shown in Fig. S2.† For both particles' sizes, the distinctive features of polystyrene infrared spectrum reported by Krimm[33] were detected. The strongest peaks at 696 and 753 cm^{-1} are associated with out-of-plane ring deformations, while peaks at 1492 and 1601 cm^{-1} are assigned to in-plane ring deformation.[33] Regarding the CH stretching region, at 2850 and 2919 cm^{-1} there are, respectively, the symmetric and asymmetric CH_2 stretching, and at 3025 cm^{-1} the stretching of aromatic CH.[33] In the spectrum of nPS it was possible to

observe two bands, not belonging to PS infrared spectrum. We may tentatively assign these bands, precisely at 1220 and 1697 cm^{-1}, to the surfactant and the fluorescent dye, present in the nanoparticles suspension formulation. Regarding the peak at 1220 cm^{-1}, it can be assigned to the antisymmetric stretching of OSO_3^- group of sodium dodecyl sulfate (SDS),[34] confirming the information about chemical nature of surfactant provided by particles' manufacturer. However, some fluorescent dyes also contain sulfate groups. Regarding the peak at 1697 cm^{-1}, it might be due to the fluorescent dye incorporated into the PS particles. A numerous class of common red dyes, rhodamines and other xanthene derivatives, have in their chemical structure carbonyl groups and conjugated rings, which can vibrate at wavenumber close to 1700 cm^{-1}.[35]

Interestingly, we noted that bands at 1220 and 1697 cm^{-1} were absent in the ATR-FTIR spectrum of smPS particles. The concentration of surfactant, needed to keep particles in suspension, was quite different for the two PS particles sizes (close to five times larger for smaller polystyrene particles). As a consequence, the very small amount of surfactant in the smPS stock solution, differently from nPS solution, was below the detection limit and was not detected. A similar hypothesis should be valid for different content of fluorescent dye. No infrared signal from preservative was detected in both particles' spectra (sodium azide has a strong band around 2040 cm^{-1}, region not shown in Fig. S2†), confirming its extremely low amount in the suspensions.

3.2 Physiological parameters

Seeds of *C. endivia* have a rod shape, with the two axes of 3 and 1 mm, respectively.

Germination percentage (Fig. 1a) evidenced no effect induced by smPS, whereas a significant impairment at 7 days with 1 g L^{-1} nPS treatment was observed; the effect disappeared after 14 days. A similar delay effect of different size particles was reported in *Lepidium sativum*.[14]

The length of the root and shoot did not appear to be significantly affected by all the treatments either at 7 or 14 days. The only exception was observed for the 1 g L^{-1} of nPS treatment at 7 days, in which both the length of the root and of the shoot were severely reduced to half than the respective control (Fig. 1b and c) but also in this case the effect disappeared at 14 days. No effect of treatment with 100 nm nPS particles was also reported on germination of *Triticum aestivum* in the range 0.01–10 g L^{-1} concentration, the growth of seedlings being enhanced.[36]

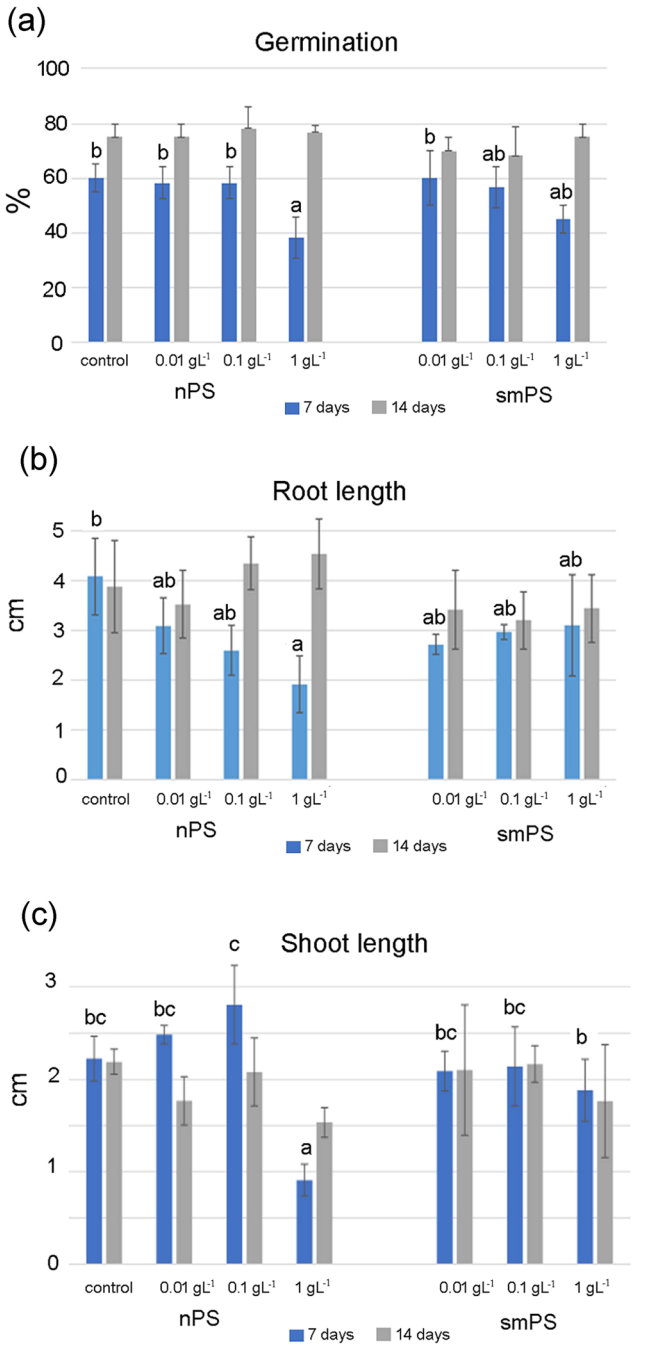

Fig. 1 Germination percentage (a), root length (b) and shoot length (c) of control and 0.01, 0.1, 1 g L^{-1} nPS and smPS treated seedlings of *Cichorium endivia*, of 7 and 14 days. Data are the average of three separate experiments ± SD. Different letters indicate significant differences among control and treatments at $P \leq 0.05$ for each time of germination. Lower case letters: seedlings of 7 days.

3.3 Cytogenetic analysis

Previous cytogenetic evaluations for *C. endivia* using fluorescent staining and cytogenetic markers reported the diploid number $2n = 18$ for this species, the genome being characterized by very small chromosomes difficult to analyze by light microscope. For this reason, Feulgen stained root meristems were also observed with fluorescence microscope at 560 nm, wavelength specific for pararosaniline.[37]

Cytological analysis on PS particles treated roots (Fig. 2) indicated no inhibitory effects of mitotic activity at the different concentrations both in nPS and smPS, but rather, mitotic index (MI) increased starting from the lowest concentration (Fig. 2a). In all smPS treatments the MI was

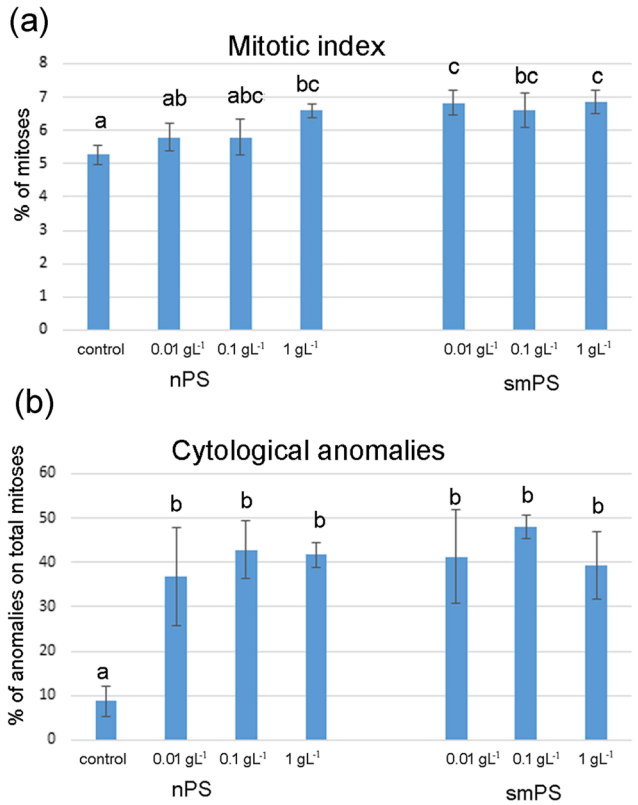

Fig. 2 Cytological analysis of 5 days control and 0.01, 0.1, 1 g L^{-1} nPS and smPS treated root meristems of *Cichorium endivia* at light microscope after Feulgen staining. Mean values of mitotic index (a); % of total cytological anomalies (abnormal metaphases + abnormal ana/telophases) (b). Data are the average of three separate experiments ± SD. Different letters indicate significant differences among control and treatments at $P \leq 0.05$.

significantly greater than in nPS and about 20% higher than in the control. This result differed from that previously observed in *A. cepa*[16] and in *Oryza sativa*[38] in which an inhibitory effect on MI was observed starting from 0.1 g L^{-1} of nPS 50 nm, indicating that the extent of cytotoxic response may depend on the plant species.[15] It is interesting to consider the MI increase, detected in all treatments of either nPS and smPS, in respect to the shorter root length observed in particular at the nPS 1 g L^{-1}.

Table S2† and Fig. 2b showed cytological analysis considering the frequencies of mitotic phases in the different treatments. Both nPS and smPS treated root meristems had a significant increase of abnormal mitoses in respect to the control.

Results from Table S2† highlighted the variation of the different mitotic phases in respect to the control. In all the PS treatments normal prophases significantly decreased from 42.6% of control to 22.6% and 16.8% in 0.1 g L^{-1} nPS and smPS, respectively. Normal metaphases significantly decreased from 25.6% (control) to 10.4% in 0.1 g L^{-1} nPS and 12.5% in 1 g L^{-1} smPS. Abnormal metaphases and abnormal anaphases increased significantly in all treatments. The analysis of the frequencies of abnormal mitotic phases highlighted that the various treatments were significantly different from the control, but were not significantly different from each other, the root meristems from smPS 0.1 g L^{-1} treatment showing the greater percentage (48%) of cytogenetic abnormalities (Fig. 2b). These anomalies could be caused by mitotic spindle failure and malfunction giving origin to c-metaphases (colchicine like metaphases in which mitotic spindle is not formed), or by the loss of one or more chromosomes (lagging chromosomes), as a consequence of the impairment of kinetochore stable attachment to spindle microtubules. Moreover, breaks or alterations of the chromosomal structures, clastogenic effect, could result in preventing chromosomes normal behaviour during mitotic division, with the formation of sticky chromosomes, chromosome bridges and chromosome fragments. Cytogenetic anomalies derived from mitotic spindle defects and clastogenic effect could generate the formation of micronuclei, their presence being a marker of DNA damage and genotoxicity.[16] Normal prophases, metaphases and anaphases/telophases were observed in control roots (Fig. S3†). C-metaphases (Fig. 3a), sticky chromosomes at metaphase (Fig. 3b), chromosome bridges at ana-telophases (Fig. 3c and d), lagging chromosomes at anaphases (Fig. 3e) was the most frequent cytological aberration. Micronuclei were seldom observed (Fig. 3f).

In *Vicia faba* nPS caused higher genotoxic and oxidative damage than microparticles, even if the latter was able to reduce plant growth, probably by altering the uptake of water and nutrients from soil.[11] Phytotoxicity, cytotoxicity, genotoxicity, and oxidative damages induced by nanoparticles of polystyrene have been also reported in *A. cepa*[16] and in *O. sativa* during early developmental stages.[39] Conflicting results were found by Lian *et al.*[36] in wheat, in which nanoparticles 100 nm in the concentration range of 0.01–10 g L^{-1} did not disturb seed germination, but rather increased root elongation, biomass, carbon and nitrogen content, partially reducing the accumulation of some micronutrients.

In the literature it has been highlighted that the presence of preservatives in commercial nanoparticles' solutions could alter toxicity results, due to biocidal effect of NaN_3.[40] Regarding this point, the concentration of sodium azide (<0.05% azide in the stock solutions) in our experiments were in the range of 0.007 mM (corresponding to 0.01 g L^{-1}) to a maximum of 0.7 mM (corresponding to 1 g L^{-1} suspension). These concentrations were always lower than those indicated in toxicological studies in plants.[41,42]

3.4 Imaging of fluorescent polystyrene particles

The imaging of fluorescent polystyrene particles evidenced that in 7 days seedlings treated with nPS particles fluorescence was evident at the level of root hairs and weakly present in the cells of the meristematic area (Fig. 4a). Moreover, fluorescence was observed in the rhizodermis cells and in the root vascular bundles (Fig. 4b), but not in the hypocotyl (Fig. 4c) independently of treatments. In 14 days

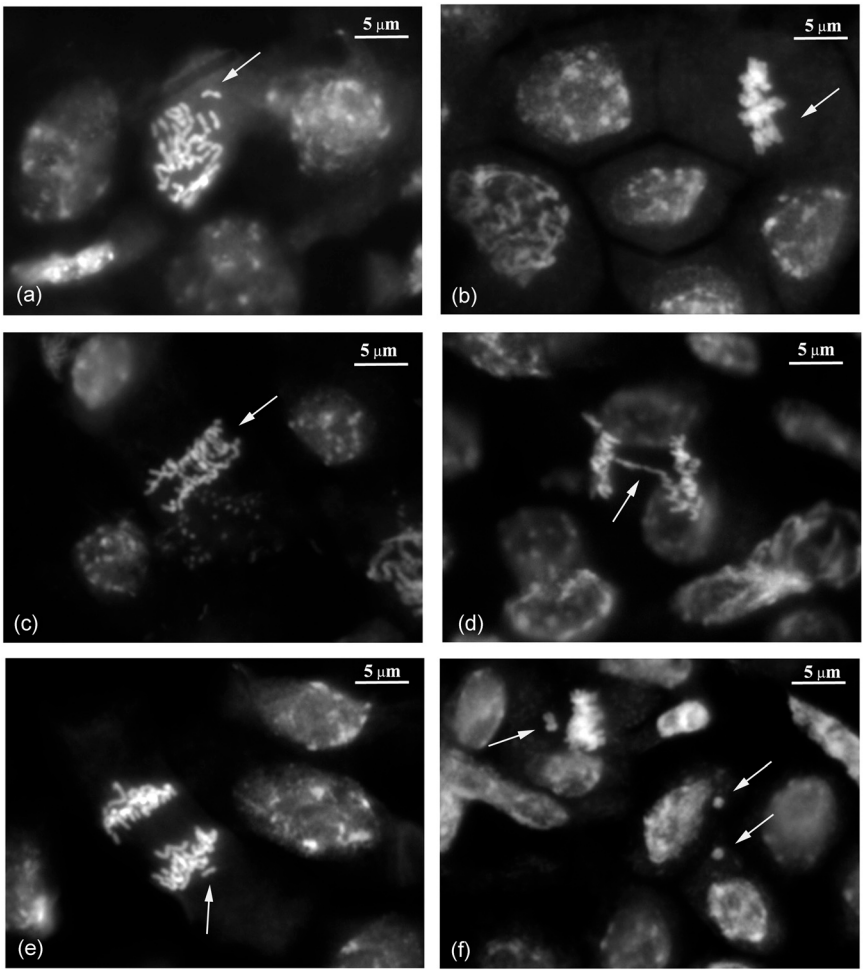

Fig. 3 Cytological aberration of 5 days 0.01, 0.1, 1 g L^{-1} nPS and smPS treated root meristems of *Cichorium endivia* detected at fluorescence microscope after Feulgen staining. C-metaphases nPS 0.01 g L^{-1} (a); sticky chromosomes at metaphase smPS 0.01 g L^{-1} (b); chromosome bridges at ana-telophases nPS 0.1 g L^{-1} (c); nPS 1 g L^{-1} (d); lagging chromosomes at anaphases smPS 1 g L^{-1} (e); micronuclei smPS 0.1 g L^{-1} (f).

seedlings, fluorescence was evident in the vascular bundles of the root but less intense in the hypocotyl (Fig. 4d), although sharper with increasing concentration of the treatments.

On the contrary, in 7 days seedlings treated with smPS particles, little fluorescence was observed inside the root near the rhizodermis and in vascular bundles (Fig. 4e).

In 14 days seedlings fluorescence was observed in rhizodermis cells and in cortical cells near rhizodermis, and weakly in vascular bundles of the roots (Fig. 4f), but less in the hypocotyl independently from the concentration of the treatments. Our results were in contrast with previous observation in Arabidopsis (*Arabidopsis thaliana*) and wheat (*Triticum aestivum*) in which either fluorescent nano and microplastics were not adsorbed by roots but were associated and accumulated at root surface and cap cells. Anyway, it has to be considered that experimental conditions using negatively-charged, 40 nm and 1 μm fluorescently-labeled polystyrene spheres, in agar growth media containing plastic spheres at 0.029 g L^{-1}, were completely different from our system.[43]

No detectable fluorescence was observed at the specific excitation wavelengths used for the nPS and smPS particles in control seedling tissues. Furthermore, leaching of fluorescent dye is strongly hindered, due to incorporation of fluorophore inside the polymer matrix. Thus, dye leaching from PS particles is prevented in aqueous solution. The specific architecture of PS particles avoids the possibility of misconceiving fluorescence signal, coming from leached fluorophore, as revealed by Catarino *et al.*[44] for PS particles with fluorescent dye adsorbed onto particles' surface. Further, we stress again that PS dissolution and subsequent leaching of fluorophore is possible in solvents like aromatic hydrocarbons (methyl ethyl ketone, benzene, *etc.*), conditions that are not encountered in our experiments. Schür *et al.* too,[45] suggested being cautious operating with fluorescent nanoparticles and do not rely solely on fluorescence to assess translocation of nanoparticles. In our multidisciplinary approach, as exposed in the next sections, the results obtained *via* fluorescence microscopy are confirmed and reinforced by infrared spectroscopy and transmission electron microscopy.

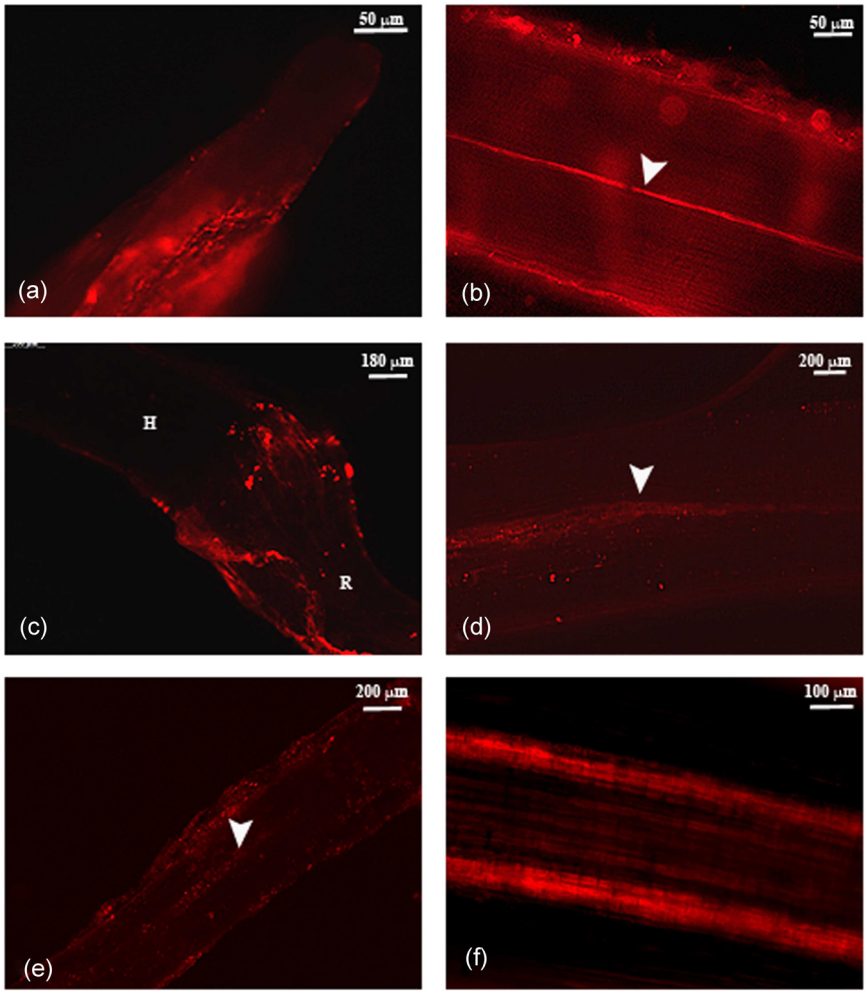

Fig. 4 Fluorescence microscope images of nPS and smPS treated seedlings of *Cichorium endivia*, of 7 and 14 days. Roots of 7 days treated with nPS 1 g L^{-1}, the arrow head indicates a vascular bundle (a and b); root–hypocotyl of 7 days treated with nPS 0.1 g L^{-1} (c); hypocotyl of 14 days treated with nPS 0.1 g L^{-1} (d); root of 7 days treated with smPS 0.01 g L^{-1} (e); root of 14 days treated with smPS 1 g L^{-1} (f). R, root; H, hypocotyl.

3.5 Attenuated Total Reflection (ATR) Fourier-Transform Infrared Spectroscopy (FTIR)

The FTIR technique has been established as an effective tool for chemical analysis of biological material,[46] being a rapid, inexpensive, and non-invasive method for obtaining chemical characteristics and composition of samples, through the identification of the main functional groups and chemical bonds present in molecules of biological interest.[46,47] Due to ease of sample preparation and versatility, ATR has become a widespread characterization tool in biological studies,[48] as well as in many branches of polymer science, *e.g.* analysis of microplastics.[49]

In this study ATR-FTIR were acquired for the separated phases of control and 1 g L^{-1} nPS and smPS seedlings treated 14 days. The extraction protocol has efficiently sorted out the polymer matter in the organic phase, together with other lipophilic compounds. Indeed, no signatures of polystyrene were visible in the ATR spectra of the interface or aqueous phase (Fig. S4†). The extraction procedure has not altered the results, in fact spectra of Fig. S5† – spectra collected on ether extraction from nPS and smPS stock solution – displayed the same infrared features of Fig. S2,† confirming that the extraction with ether dissolves the polymer, without any substantial alteration.

The infrared spectra obtained from the organic solvent phase evidenced that polystyrene was clearly visible only in the spectrum of nPS (Fig. 5). Compared to control spectrum, peaks at 698 and 754 cm^{-1}, due to PS out-of-plane ring deformations, emerge in the nPS spectrum. Furthermore, a tiny but well resolved peak at 3024 cm^{-1}, due to aromatic CH stretching, was distinguishable in the nPS spectrum. The same peaks did not appear in the smPS spectrum, probably being the amount of smPS particles absorbed by the seedling below the detectability limit (Fig. 5). It is noteworthy to observe that peak positions and relative intensities were very similar to the ones spotted in nPS and smPS spectra. The nature of monosubstituted benzene and the coupling with polymer backbone determined the precise peak position and absorbance[33] in the spectra of polystyrene and differentiated

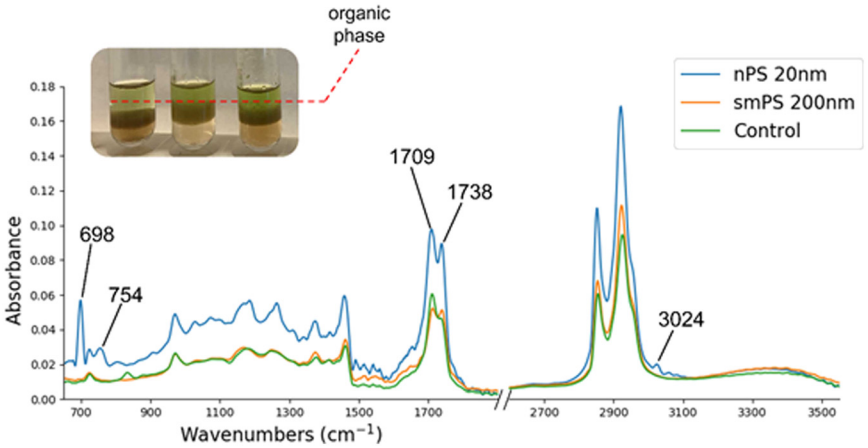

Fig. 5 ATR-FTIR spectra of control and 1 g L^{-1} nPS and smPS treated seedlings of *Cichorium endivia*, of 14 days. Infrared spectrum of seedlings treated with nPS shows signatures of polystyrene at 698, 754 and 3024 cm^{-1}. The inset shows the test tubes of a set of samples after extraction procedure.

it from styrene or other styrene containing compound. Therefore, due to high specificity of infrared spectroscopy to chemical structure, the observed results were further evidence of internalization of polystyrene. Moreover, ATR-FTIR demonstrated that the uptake of PS particles occurred more easily and in a larger amount with nPS treatment. Spectra of bands other than polymer ones were shown in Fig. 5. An intense double peak at 1709 and 1738 cm^{-1} was observed in the spectra of nPS and smPS particles. The same doublet showed up in the spectrum of control sample, although with a very different relative intensity of the two peaks. Indeed, in the control spectrum the peak at 1738 cm^{-1} appeared like a shoulder, while it was clearly split in the spectra of samples treated with polymer particles. The extraction protocol brought in the organic phase other compounds present in the biological samples. The doublet around 1700 cm^{-1} may be assigned, in part or totally, to chlorophyll. Either chlorophyll a and chlorophyll b have a strong ester absorption at 1735 cm^{-1}, a free ketone carbonyl absorption at 1703–1695 cm^{-1} and a coordinated ketone (chlorophyll in dimer form) absorption around 1652 cm^{-1}.[50,51] However, precise peak position and intensity might be affected by several factors: chlorophyll type, solvent, presence of nucleophile molecules, hydrogen bonding.[50] Greenish colour of the ether solution is further evidence that chlorophyll may be dissolved in the organic phase. However, several more substances might be present, with carbonyl groups absorbing in the same spectral region, *e.g.* carotenoids.[52] For these reasons, it was difficult to clarify the different lineshape existing between the control and the treated samples. Nevertheless, it is noteworthy that also spectrum of smPS showed an altered balance of pigments, although smPS polymer particles were observed less frequently into plant structures. Such evidence was confirmed by results reported in Content of photosynthetic pigments section.

3.6 Transmission Electron Microscope (TEM) observations

The cortical cells of the control roots were large with a large central vacuole. In the thin layer of cytoplasm few organelles were present (Fig. S6†). On the contrary, in both nPS and smPS treated roots, cells appeared in slight plasmolysis with nPS detectable in the space between plasmalemma and cell wall and in vacuoles as single particles, or in the form of small aggregates (Fig. 6a and b). The shoot cells ultrastructure showed cells with large electron transparent vacuoles, cytoplasm rich in organelles as mitochondria, chloroplast with numerous and well-structured thylakoids, and peroxisomes with large crystals (Fig. 6c). The nPS treated shoot cells appeared often in more or less intense plasmolysis (Fig. 6d). In the cytoplasm, the chloroplasts showed often disrupted thylakoids membranes and numerous not well recognizable organelles were evident (Fig. 6d). The nPS were present as small aggregates in the vacuoles (Fig. 6e). In smPS treated shoot, rare particles were detected in vacuoles and in the space between plasmalemma and cell wall in weakly plasmolyzed cells (Fig. 6f). These results corroborate the findings of infrared spectroscopy and fluorescence microscopy, evidencing the effectiveness of integrating several characterization techniques for the study of nanoparticles translocation.

Recently, some papers have demonstrated that nanoparticles of polystyrene could be taken up by crop plants and translocated from root to shoot.[36,39,53,54] The fluorescence observed in the root hairs, in the root vascular bundles of 7 day seedlings and in the hypocotyl of the 14 day seedlings treated with nPS, allowed to suppose that the nPS particles could enter the root and reach the shoot following the xylematic flow and the transpiration stream, that are more intense during plantlet development.[55] On the contrary, the localization of smPS particles fluorescence was mainly near rhizodermis and weak in the vascular bundles of the

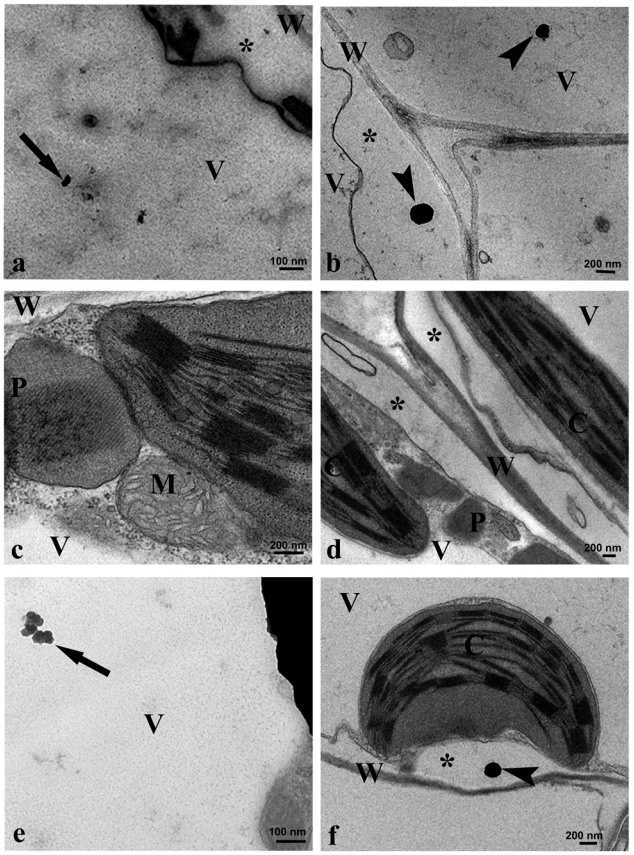

Fig. 6 TEM images of control and 1 g L^{-1} nPS and smPS treated seedlings of *Cichorium endivia*, of 14 days. Vacuole of cell of nPS treated root, the arrow indicates nPS particle (a); vacuoles of cell of smPS treated root, the arrowheads indicate smPS particles (b); portion of cytoplasm of control shoot (c); portion of cytoplasms of nPS treated shoot cells (d); vacuole of nPS treated shoot cell, the arrow indicates nPS particles aggregate (e); portion of cells of smPS treated shoot, the arrowhead indicates smPS particle (f). Asterisks indicate plasmalemma wall detachment. C, chloroplast; M, mitochondrion; P, peroxisome; V, vacuole; W, cell wall.

root only in 14 days seedlings. This could reflect the difficulty of these larger particles to enter the root and to move within the tissues.[56] Results were consistent with ATR-IR measurements confirmed that *C. endivia* seedlings absorbed more easily nPS.

Worthy of attention was the presence of plasmolysis in all tissues of all treated samples that could be related to a reduced water absorption. In different work it was reported that the high plastic concentration limited water absorption necessary for the normal imbibition, germination and primary root growth.[10,14] Moreover, plastics accumulating near the root tip of terrestrial plants, can limit water absorption through the blockage of cell wall pores.[11] On this basis, the inhibitory effects on germination and roots lengthening observed at 7 days in highest treatment may be due to an impairment to cell distension rather than cell division. This idea was supported by the fact that cytological analysis indicated no significant effect on MI of the treated roots.

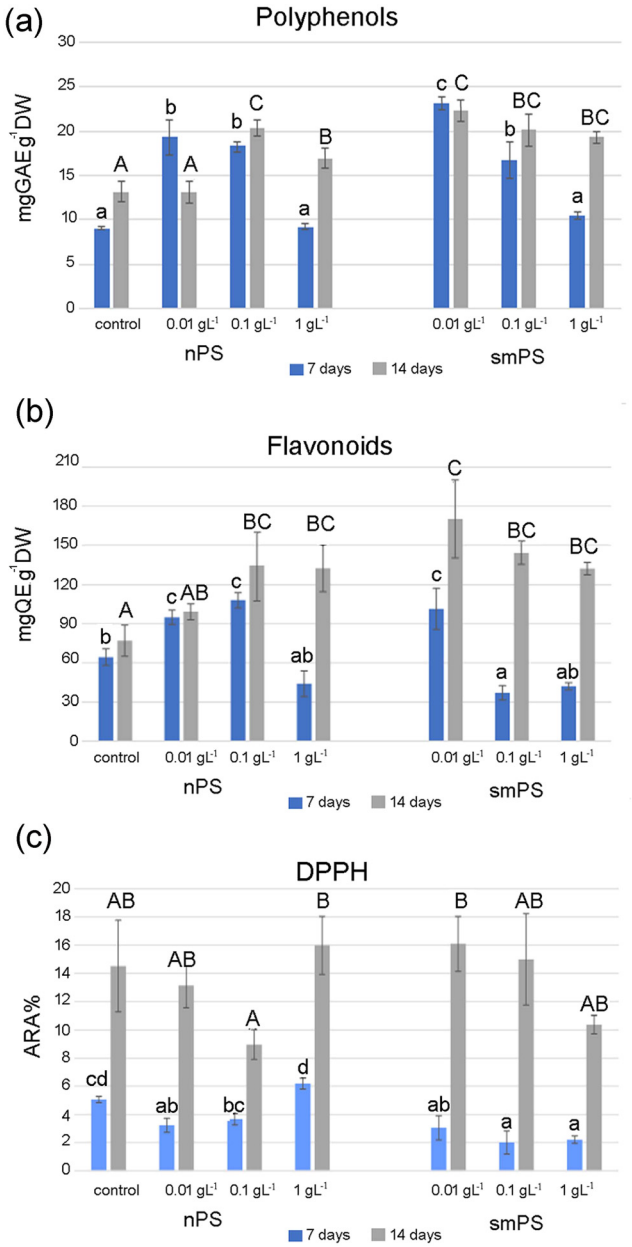

Fig. 7 Content of polyphenols (a), of flavonoids (b) and antioxidant activity (c) in control and 0.01, 0.1, 1 g L^{-1} nPS and smPS treated seedlings of *Cichorium endivia*, of 7 and 14 days. Data are the average of three separate experiments ± SD. Different letters indicate significant differences among control and treatments at $P \leq 0.05$ for each time of germination. Lower case letters: 7 days seedlings; capital letters: 14 days seedlings. Content of polyphenols is expressed as mg gallic acid equivalent (GAE) g^{-1} DW, content of flavonoids as mg quercetin equivalent (QE) g^{-1} DW and antiradical activity (ARA) expressed as percentage inhibition of the DPPH˙ radical.

3.7 Content of phytochemicals and antioxidant activity

The total polyphenols content (TPC) in 7 days control seedlings was about 9 mg GAE g^{-1} DW and significantly increased at the concentration of 0.01 and 0.1 g L^{-1} either for nPS and smPS. At the concentration of 1 g L^{-1} the TPC was

instead similar to that of control for particles of both sizes (Fig. 7a). In 14 days treated seedlings, the TPC was always significantly higher than control for both nPS and smPS in a range of 20 mg GAE g^{-1} DW, except for 0.01 g L^{-1} nPS which had a value similar to control.

The total flavonoids content (TFC) in 7 days control seedlings was about 60 mg QE g^{-1} DW and increased significantly to 90 mg QE g^{-1} DW at 0.01 and to 110 mg QE g^{-1} DW at 0.1 g L^{-1} nPS treatment and 0.01 g L^{-1} smPS. A decrease at 1 g L^{-1} nPS and at 0.1 and 1 g L^{-1} smPS was observed. In 14 days seedlings, the flavonoids content increased significantly at all the treatments up to a level ranging from to 120 to 160 mg QE g^{-1} DW (Fig. 7b).

Antioxidant activity was evaluated by the 2,2-diphenyl-1-picrylhydrazyl (DPPH˙) test, that is specific for antioxidant molecules acting by transfer of hydrogen or electrons (radical quenching). The antiradical activity (ARA) of control *C. endivia*, measured at 7 days was about 5% and decreased in all the treatments of nPS and smPS except for 0.1 and 1 g L^{-1} nPS (Fig. 7c). In 14 days seedlings, the ARA ranged between 14–16% in control and all the treatments with no significative differences (Fig. 7c).

The detected pattern for TPC and TFC could be explained as a response to the stress induced by germination in presence of PS particles at 0.01 and 0.1 g L^{-1}, while the concentration of 1 g L^{-1} impairs antioxidant compounds production. At 14 days the increase was present also at the highest concentration. The increase in the antioxidant activity during the germination detected in control and treated seedlings at 14 days in respect to 7 days, was in agreement with previous works in which DPPH˙ analysis in radish, broccoli and sunflowers[57] and black kale[58] evidenced a general higher antioxidant capacity in young sprouts, supposed to be related to the rise in the content of antioxidant compounds, such as vitamins, polyphenols, flavonols and flavonoids.

3.8 Content of photosynthetic pigments

In 14 days seedlings, photosynthetic pigments *i.e.* chlorophyll a (chl a), chlorophyll b (chl b), total chlorophyll (chl tot) and carotenoids (car) were evaluated in the green portion of the seedlings, which at this stage is represented by photosynthetic cotyledons and primary leaves. Exposure for 14 days to different concentrations of nPS and smPS particles reflected a statistically significant different content of photosynthetic pigments in *C. endivia* (Fig. 8). In all the treated samples, the content of chl a was significantly higher than control (3.5 m g^{-1} DW) but at 1 g L^{-1} concentration, the chl a level decreased both in nPS and smPS in respect to lower concentration treatments. In particular, chl a content was always higher than chl b, as expected. The chl b content (1.1 mg g^{-1} DW in the control), increased in all treatments, except for 0.01 g L^{-1} nPS, keeping constant to a level around 3 mg g^{-1} DW. A similar increasing trend was observed for chl tot (Fig. 8a).

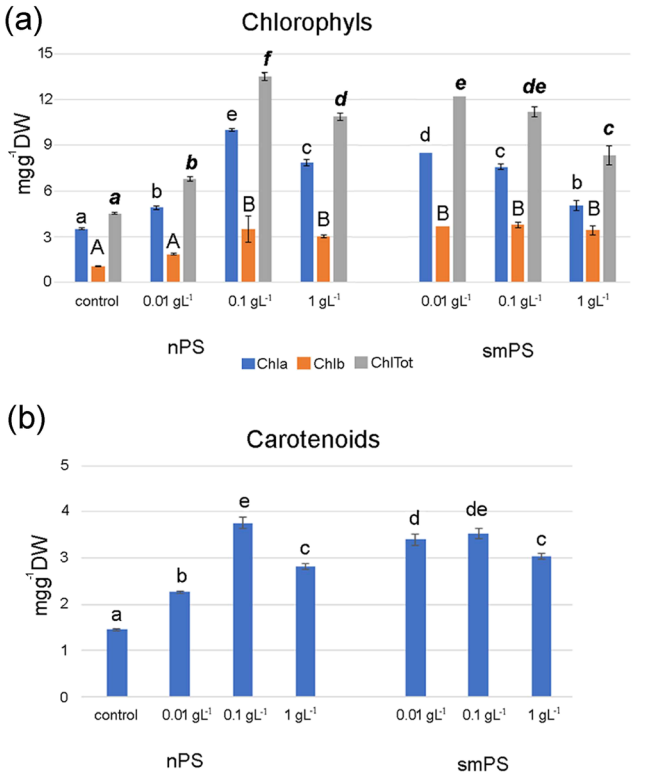

Fig. 8 Content of photosynthetic pigments (chlorophyl a, chlorophyl b, chlorophyl total) (a) and carotenoids (b) in control and 0.01, 0.1, 1 g L^{-1} nPS and smPS treated seedlings of *Cichorium endivia*, of 14 days. Data are the average of three separate experiments ± SD. Different letters indicate significant differences among control and treatments at $P \leq 0.05$. In figure (a): lower case letters: chl a, capital letters: chl b, italics bold: chl tot. Content is expressed as mg g^{-1} DW.

Conflicting results were reported in several papers: environmental stresses damaging the biosynthesis of chlorophylls, leading to a decrease in photosynthesis efficiency,[59] no effect on the chlorophyl content was observed in *Spirodela polyrhiza* plants treated with micro and nanoplastics.[60] High chl a level was observed in *Triticum aestivum* plants treated with micro polyethylene (PE) added with polyvinylchloride (PVC)[12] and in *Lepidium sativum* treated with PE, PP (polypropylene), and PVC microplastics.[61]

In seedlings of 14 days, the content of carotenoids significantly increased in all nPS and smPS treatments (Fig. 8b), the level being similar to that of chl b. In the present study, the photosynthetic pigments increase following nPS and smPS treatments was in accordance to results in other species, the effect extent depending on size and concentration of the particles.[54,61]

4. Conclusions

The use of different techniques and tools used in the present research allowed to highlight and clarify the effects of the stress induced by the polystyrene particles. By the physiological data, it was demonstrated that in *C. endivia* seed germination and seedling elongation were weakly

influenced by the treatments with the exception of the 1 g L^{-1} concentration at 7 days. Since treated seedling at 14 days did not show significant differences with the control, a physiological recovery in terms of plant growth could be hypothesized.

The internalization of nPS and smPS observed with TEM and characterized with FTIR, led to biochemical, cytogenetic and ultrastructural consequences. In fact, an increase in the concentration of antioxidants molecules was detected as probable effect of the stress induced by the particles. Cytogenetic anomalies and damages detected at the ultrastructural level such as the alteration of the thylakoid membranes, especially in the samples treated with nPS, were in line with the presence of nPS particles in the tissues, demonstrated by fluorescence microscopy and FTIR analysis. In conclusion, damages induced by polystyrene particles could be the trigger of deeper consequences on the development of seedlings, thus impairing adult plant formation. The presence of nPS and smPS in the tissues of *C. endivia* could suggest their entrance in the food chain.

Author contributions

L. Bellani, S. Muccifora and L. Giorgetti conceived and designed the study. L. Bellani and S. Muccifora performed the biochemical and Transmission Electron Microscope analysis; L. Giorgetti the cytogenetic analysis; M. Corsini and G. Di Florio the infrared spectroscopy. All the authors analysed the results and wrote the manuscript.

Conflicts of interest

The authors declare non competing financial interest.

Acknowledgements

This work was financed by funding of University of Siena (PSR) and supported by National Research Council of Italy. G. Di Florio acknowledges Senior Professor Riccardo Basosi for the constant mentoring and for pushing him to explore connections between physical chemistry, material science and environmental problems. The authors thank Prof. Andrea Massimo Atrei for performing Dynamic Light Scattering measurements on PS particles stock solutions.

References

1 *Plastic Europe 2020*, **https://plasticseurope.org/wp-content/uploads/2021/09/Plastics_the_facts-WEB-2020_versionJun21_final.pdf**.
2 *ISO/TS 80004–2:2015: Nanotechnologies – Vocabulary – Part 2: Nano-objects*, The International Organization for Standardization, Geneva, 2015.
3 Y. S. K. De Silva, U. M. Rajagopalan and H. Kadono, Microplastics on the growth of plants and seed germination in aquatic and terrestrial ecosystems, *Global J. Environ. Sci. Manage.*, 2021, **7**, 347–368.
4 K. Syberg, F. R. Khan, H. Selck, A. Palmqvist, G. T. Banta, J. Daley, L. Sano and M. B. Duhaime, Microplastics: addressing ecological risk through lessons learned, *Environ. Toxicol. Chem.*, 2015, **34**, 945–953.
5 A. Mateos-Cárdenas, F. N. A. M. van Pelt, J. O'Halloran and M. A. K. Jansen, Adsorption, uptake and toxicity of micro- and nanoplastics: Effects on terrestrial plants and aquatic macrophytes, *Environ. Pollut.*, 2021, **284**, 117183.
6 A. A. Horton, A. Walton, D. J. Spurgeon, E. Lahive and C. Svendsen, Microplastics in freshwater and terrestrial environments: Evaluating the current understanding to identify the knowledge gaps and future research priorities, *Sci. Total Environ.*, 2017, **586**, 127–141.
7 E. Herta Lwanga, J. Mendoza Vega, V. Ku Quej, J. de los Angeles Chi, L. Sanchez Del Cid, C. Chi, G. Escalona Segura, H. Gertsen, T. Salánki, M. van der Ploeg, A. A. Koelmans and V. Geissen, Field evidence for transfer of plastic debris along a terrestrial food chain, *Sci. Rep.*, 2017, **7**, 14071.
8 Y. Chae and Y. J. An, Nanoplastic ingestion induces behavioral disorders in terrestrial snails: trophic transfer effects via vascular plants, *Environ. Sci.: Nano*, 2020, **7**, 975–983.
9 U. Rozman, T. Turk, T. Skalar, M. Zupančič, N. Čelan Korošin, M. Marinšek, J. Olivero-Verbel and G. Kalčíková, An extensive characterization of various environmentally relevant microplastics - Material properties, leaching and ecotoxicity testing, *Sci. Total Environ.*, 2021, **773**, 145576, DOI: **10.1016/j.scitotenv.2021.145576**.
10 G. Kalčíková, G. A. Žgajnar, A. Kladnik and A. Jemec, Impact of polyethylene microbeads on the floating freshwater plant duckweed *Lemna minor*, *Environ. Pollut.*, 2017, **230**, 1108–1115.
11 X. Jiang, H. Chen, Y. Liao, Z. Ye, M. Li and G. Klobučar, Ecotoxicity and genotoxicity of polystyrene microplastics on higher plant *Vicia faba*, *Environ. Pollut.*, 2019, **250**, 831–838.
12 Y. Qi, X. Yang, P. A. Mejia, E. Herta Lwanga, N. Beriot, H. Gertsen, P. Garbeva and V. Geissen, Macro- and micro-plastics in soil-plant system: Effects of plastic mulch film residues on wheat (*Triticum aestivum*) growth, *Sci. Total Environ.*, 2018, **645**, 1048–1056.
13 B. Boots, C. W. Russell and D. S. Green, Effects of Microplastics in Soil Ecosystems: Above and Below Ground, *Environ. Sci. Technol.*, 2019, **53**, 11496–11506.
14 T. Bosker, J. L. Bouwman, R. N. Brun, P. Behrens and G. M. Vijver, Microplastics accumulate on pores in seed capsule and delay germination and root growth of the terrestrial vascular plant *Lepidium sativum*, *Chemosphere*, 2019, **226**, 774–781.
15 S. van Weert, E. P. Redondo-Hasselerharm, J. N. Diepens and A. A. Koelmans, Effects of nanoplastics and microplastics on the growth of sediment-rooted macrophytes, *Sci. Total Environ.*, 2019, **654**, 1040–1047.
16 L. Giorgetti, C. Spanò, S. Muccifora, S. Bottega, F. Barbieri, L. Bellani and M. Ruffini Castiglione, Exploring the interaction between polystyrene nanoplastics and *Allium cepa* during germination: Internalization in root cells,

induction of toxicity and oxidative stress, *Plant Physiol. Biochem.*, 2020, **149**, 170–177.

17 A. A. De Souza Machado, W. C. Lau, W. Kloas, J. Bergmann, B. J. Bachelier, E. Faltin, R. Becker, S. A. Görlich and C. M. Rillig, Microplastics Can Change Soil Properties and Affect Plant Performance, *Environ. Sci. Technol.*, 2019, **53**, 6044–6052.

18 S. Maity and K. Pramanick, Perspectives and challenges of micro/nanoplastics-induced toxicity with special reference to phytotoxicity, *Global Change Biol.*, 2020, **26**, 3241–3250.

19 K. Kik, B. Bukowska and P. Sicińska, Polystyrene nanoparticles: Sources, occurrence in the environment, distribution in tissues, accumulation and toxicity to various organisms, *Environ. Pollut.*, 2020, **262**, 114297.

20 G. Oliveri Conti, M. Ferrante, M. Banni, C. Favara, I. Nicolosi, A. Cristaldi, M. Fiore and P. Zuccarello, Micro- and nano-plastics in edible fruit and vegetables. The first diet risks assessment for the general population, *Environ. Res.*, 2020, **187**, 109677.

21 S. Nandagopal and B. D. Ranjitha Kumari, Phytochemical and antibacterial studies of chicory (*Cichorium intybus* L.) – a multipurpose medicinal plant, *Adv. Biol. Res.*, 2007, **1**, 17–21.

22 C. Cavin, M. Delannoy, A. Malnoe, E. Debefve, A. Touche, D. Courtois and B. Schilter, Inhibition of the expression and activity of cyclooxygenase-2 by chicory extract, *Biochem. Biophys. Res. Commun.*, 2005, **327**, 742–749.

23 S. Saggu, M. I. Sakeran, N. Zidan, E. Tousson, A. Mohan and H. Reheman, Ameliorating effect of chicory (*Cichorium intybus* L.) fruit extract against 4-tert-octylpenol induced liver injury and oxidative stress in male rats, *Food Chem. Toxicol.*, 2014, **72**, 138–146.

24 M. Al-Sid-Cheikh, S. J. Rowland, K. Stevenson, C. Rouleau, T. B. Henry and R. C. Thompson, Uptake, whole-body distribution, and depuration of nanoplastics by the scallop *Pecten maximus* at environmentally realistic concentrations, *Environ. Sci. Technol.*, 2018, **52**, 14480–14486.

25 A. Wahl, C. Le Juge, M. Davranche, H. El Hadri, B. Grassl, S. Reynaud and J. Gigault, Nanoplastic occurrence in a soil amended with plastic debris, *Chemosphere*, 2021, **262**, 127784, DOI: **10.1016/j.chemosphere.2020**.

26 D. Hayes, *Micro- and Nanoplastics in Soil: Should We Be Concerned?*, Report no. PA-2019-01, USDA, 2019, **https://Biodegradablemulch.org**.

27 M. Milosevic, Internal Reflection and ATR Spectroscopy, *Appl. Spectrosc. Rev.*, 2004, **39**, 365–384, DOI: **10.1081/ASR-200030195**.

28 M. J. Karnovsky, A formaldehyde-glutaraldehyde fixative of high osmolality for use in electron microscopy, *J. Cell Biol.*, 1965, **27**, 137–138.

29 V. L. Singleton and J. A. Rossi, Colorimetric of total phenols with phosphomolybdic-phosphotungstic acid reagents, *Am. J. Enol. Vitic.*, 1965, **16**, 144–158.

30 D. Heimler, P. Vignolini, M. G. Dini, F. F. Vincieri and A. Romani, Antiradical Activity and Polyphenol Composition of Local Brassicaceae Edible Varieties, *Food Chem.*, 2006, **99**, 464–469.

31 S. Boudjou, B. D. Oomah, F. Zaidi and F. Hosseinian, Phenolics content and antioxidant and anti-inflammatory activities of legume fractions, *Food Chem.*, 2013, **138**, 1543.

32 H. K. Lichtenthaler, Chlorophylls and carotenoids: Pigments of photosynthetic biomembranes, *Methods Enzymol.*, 1987, **148**, 350–382, Academic Press.

33 S. Krimm, Infrared spectra of high polymers, in *Fortschritte Der Hochpolymeren-Forschung. Advances in Polymer Science*, Springer, Berlin, Heidelberg, 1960, vol. 2/1, DOI: **10.1007/BFb0050351**.

34 X. Gao and J. Chorover, Adsorption of sodium dodecyl sulfate (SDS) at ZnSe and α-Fe_2O_3 surfaces: Combining infrared spectroscopy and batch uptake studies, *J. Colloid Interface Sci.*, 2010, **348**, 167–176.

35 S. Ramos, A. F. Vilhena, L. Santos and P. Almeida, ^{1}H and ^{13}C NMR spectra of commercial rhodamine ester derivatives, *Magn. Reson. Chem.*, 2000, **38**, 475–478.

36 J. Lian, J. Wu, H. Xiong, A. Zeb, T. Yang, X. Su, L. Su and W. Liu, Impact of polystyrene nanoplastics (PSNPs) on seed germination and seedling growth of wheat (*Triticum aestivum* L.), *J. Hazard. Mater.*, 2020, **385**, 121620.

37 N. Böhm and E. Sprenger, Fluorescence cytophotometry: A valuable method for the quantitative determination of nuclear Feulgen-DNA, *Histochemie*, 1968, **16**, 100–118.

38 C. Spanò, S. Muccifora, M. Ruffini Castiglione, L. Bellani, S. Bottega and L. Giorgetti, Polystyrene nanoplastics affect seed germination, cell biology and physiology of rice seedlings in-short term treatments: evidence of their internalization and translocation, *Plant Physiol. Biochem.*, 2022, **172**, 158–166.

39 C. Q. L. Zhou, C. H. Lu, L. Mai, L. J. Bao, L. Y. Liu and E. Y. Zeng, Response of rice (*Oryza sativa* L.) roots to nanoplastic treatment at seedling stage, *J. Hazard. Mater.*, 2021, **401**, 123412.

40 O. Pikuda, E. G. Xu, D. Berk and N. Tufenkji, Toxicity Assessment of Micro- and Nanoplastics Can Be Confounded by Preservatives in Commercial Formulations, *Environ. Sci. Technol. Lett.*, 2019, **6**, 21–25.

41 F. Al-Qurainy, Effects of Sodium Azide on Growth and Yield Traits of *Eruca sativa* L., *World Appl. Sci. J.*, 2009, **7**, 220–226.

42 A. A. Abdul-Rahaman, A. A. Afolabi, D. A. Zhigila, F. A. Oladele and A. A. Al Sahli, Morpho-anatomical effects of sodium azide and nitrous acid on *Citrullus lanatus* (Thunb.) Matsum. & Nakai (Cucurbitaceae) and *Moringa oleifera* Lam. (Moringaceae), *Hoehnea*, 2018, **45**, 225–237.

43 S. E. Taylor, C. I. Pearce, K. A. Sanguinet, D. Hu, W. B. Chrisler, Y. M. Kim, Z. Wang and M. Flury, Polystyrene nano- and microplastic accumulation at *Arabidopsis* and wheat root cap cells, but no evidence for uptake into roots, *Environ. Sci.: Nano*, 2020, **7**, 1942–1953.

44 A. I. Catarino, A. Frutos and T. B. Henry, Use of fluorescent-labelled nanoplastics (NPs) to demonstrate NP absorption is inconclusive without adequate controls, *Sci. Total Environ.*, 2019, **670**, 915–920.

45 C. Schür, S. Rist, A. Baun, P. Mayer, N. B. Hartmann and M. Wagner, When Fluorescence is not a Particle: The tissue translocation of microplastic in *Daphnia magna* seems an artifact, *Environ. Toxicol. Chem.*, 2019, **38**, 1495–1503.

46 M. Baker, J. Trevisan, P. Bassan, R. Bhargava, H. J. Butler, K. M. Dorling, P. R. Fielden, S. W. Fogarty, N. J. Fullwood, K. A. Heys, C. Hughes, P. Lasch, P. L. Martin-Hirsch, B. Obinaju, G. D. Sockalingum, J. Sulé-Suso, R. J. Strong, M. J. Walsh, B. R. Wood, P. Gardner and F. L. Martin, Using Fourier transform IR spectroscopy to analyze biological materials, *Nat. Protoc.*, 2014, **9**, 1771–1791.

47 T. Durak and J. Depciuch, Effect of plant sample preparation and measuring methods on ATR-FTIR spectra results, *Environ. Exp. Bot.*, 2020, **169**, 103915.

48 B. Ribeiro da Luz, Attenuated total reflectance spectroscopy of plant leaves: a tool for ecological and botanical studies, *New Phytol.*, 2006, **172**, 305–318.

49 A. Käppler, D. Fischer, S. Oberbeckmann, G. Schernewski, M. Labrenz, K. J. Eichhorn and B. Voit, Analysis of environmental microplastics by vibrational microspectroscopy: FTIR, Raman or both?, *Anal. Bioanal. Chem.*, 2016, **408**, 8377–8391.

50 K. Ballschmiter and J. J. Katz, An Infrared Study of Chlorophyll-Chlorophyll and Chlorophyll-Water Interactions, *J. Am. Chem. Soc.*, 1969, **91**, 2661–2677.

51 L. L. Shipman, T. M. Cotton, J. R. Norris and J. J. Katz, New proposal for structure of special-pair chlorophyll, *Proc. Natl. Acad. Sci. U. S. A.*, 1976, **73**, 1791–1794.

52 T. Lorand, J. Deli, P. Molnar and G. Toth, FT-IR Study of Some Carotenoids, *Helv. Chim. Acta*, 2002, **85**, 1691–1697.

53 X. D. Sun, X. Z. Yuan, Y. Jia, L. J. Feng, F. P. Zhu, S. S. Dong, J. Liu, X. Kong, H. Tian, J. L. Duan, Z. Ding, S. G. Wang and B. Xing, Differentially charged nanoplastics demonstrate distinct accumulation in *Arabidopsis thaliana*, *Nat. Nanotechnol.*, 2020, **15**, 755–760.

54 J. Wu, W. Liu, A. Zeb, J. Lian, Y. Sun and H. Sun, Polystyrene microplastic interaction with *Oryza sativa*: toxicity and metabolic mechanism, *Environ. Sci.: Nano*, 2021, **8**, 3699–3710.

55 L. Li, Y. Luo, R. Li, Q. Zhou, W. Peijnenburg, N. Yin, J. Yang, C. Tu and Y. Zhang, Effective uptake of submicrometre plastics by crop plants via a crack-entry mode, *Nat. Sustain.*, 2020, **3**, 929–937.

56 S. Muccifora, H. Castillo-Michel, F. Barbieri, L. Bellani, M. Ruffini Castiglione, C. Spanò, A. E. Pradas del Real, L. Giorgetti and E. L. Tassi, Synchrotron Radiation Spectroscopy and Transmission Electron Microscopy techniques to evaluate TiO_2 NPs incorporation, speciation, and impact on root cells ultrastructure of *Pisum sativum* L. plants, *Nanomaterials*, 2021, **11**, 921.

57 P. Pająk, R. Socha, D. Gałkowska, J. Rożnowski and T. Fortuna, Phenolic profile and antioxidant activity in selected seeds and sprouts, *Food Chem.*, 2014, **143**, 300–306.

58 L. Giorgetti, G. Giorgi, E. Cherubini, P. G. Gervasi, C. M. Della Croce, V. Longo and L. Bellani, Screening and identification of major phytochemical compounds in seeds, sprouts and leaves of Tuscan black kale *Brassica oleracea* (L.) ssp acephala (DC) var. sabellica L., *Nat. Prod. Res.*, 2018, **32**, 1617–1626.

59 V. K. Dalal and B. C. Tripathy, Modulation of chlorophyll biosynthesis by water stress in rice seedlings during chloroplast biogenesis, *Plant, Cell Environ.*, 2012, **9**, 1685–1703.

60 L. C. Dovidat, B. W. Brinkmann, M. G. Wijver and T. Bosker, Plastic particles absorb to root of fresh water vascular plant *Spirodera polyrhiza* but do not impair growth, *Limnol. Oceanogr. Lett.*, 2020, **5**, 37–45.

61 S. Pignattelli, A. Broccoli and M. Renzi, Physiological responses of garden cress (*L. sativum*) to different types of microplastics, *Sci. Total Environ.*, 2020, **727**, 138609.

